Reduction of copper ions release by a novel ecofriendly electropolymerized nanolayer obtained from a natural compound (carvacrol)

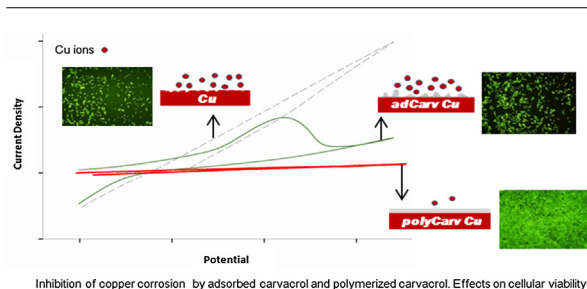M. Bertuola [a], C.A. Grillo [a], M. Fernández Lorenzo de Mele [a,b,*]

[a] Instituto de Investigaciones Fisicoquímicas Teóricas y Aplicadas (INIFTA), CONICET, Facultad de Ciencias Exactas, Departamento de Química, Universidad Nacional de La Plata, Casilla de Correo 16, Sucursal 4, 1900 La Plata, Argentina
[b] Facultad de Ingeniería, Universidad Nacional de La Plata, Calle 47 y 1, 1900 La Plata, Argentina

HIGHLIGHTS

- Carvacrol (Carv) is a natural compound, component of origanum essential oil.
- Cu corrosion in chloride medium is inhibited by treatments with Carv.
- A highly protective layer was obtained by electropolymerization of Carv (polyCarv).
- Carv adsorptive layer was not protective enough to inhibit corrosion.
- PolyCarv shows ether bonds, reduces Cu ions release and is ecofriendly.

GRAPHICAL ABSTRACT

Inhibition of copper corrosion by adsorbed carvacrol and polymerized carvacrol. Effects on cellular viability.

ARTICLE INFO

ABSTRACT

The release of copper ions by copper-containing devices, equipments and facilities represents a potential risk for biological systems. Different inhibitory treatments (CuIT) that use organic compounds have been proposed to reduce this environmental hazard but many of them are not in accordance with new regulations. The development of an ecofriendly CuIT based on the use of carvacrol, a natural phenolic compound present in essential oils, is reported here. The effects of carvacrol adsorption (adCarv) and its electropolymerization (polyCarv) were examined. Electropolymerization was attained after cycling the copper electrode in the 0.3–1.0 V potential range. Electrochemical techniques complemented by ATR-FTIR, XPS, SEM and AFM surface analyses were used to evaluate the composition and characteristics of the layers. Results demonstrated that adCarv includes cetonic structures while polyCarv additionally contains ether bonds. AFM and SEM observations showed the presence of round nanoglobules, larger for adCarv (close to 50 nm diameter). Cytotoxicity of adCarv and polyCarv layers on copper was also evaluated. The comparative analysis of both treatments revealed that polyCarv nanolayer is highly protective while the adCarv layer is weakly protective and reduction in cell viability was found. It was concluded that CuIT that leads to polyCarv nanolayer is very effective and ecofriendly.

© 2016 Elsevier B.V. All rights reserved.

1. Introduction

Due to their excellent thermal and electrical conductivity together with their simple fabrication and joining, copper and its alloys have been widely used in several industries such as pipeline,

* Corresponding author at: Casilla de Correo 16, Sucursal 4, 1900 La Plata, Argentina.
E-mail addresses: mmele@inifta.unlp.edu.ar, fernandezlorenzom@hotmail.com (M. Fernández Lorenzo de Mele).

automotive, electrical and manufacturing industries as well as in facilities that include heat exchangers, gathering pipelines, and medical devices (intrauterine devices, IUD). However, in aggressive media, deterioration of metallic materials by chemical interaction with their surrounding environments occurs [1,2]. Corrosion of metals is a form of waste that pollutes the environment. Particularly, copper ions are one of the most harmful heavy metals for aquatic ecosystems. The environmental consequences often extend far beyond the immediate issue of resource depletion. Greater awareness of detrimental consequences of corrosion will help us to preserve the environment [3]. Corrosion processes occurring in copper-containing devices, equipments and facilities lead to the release of copper ions in the surroundings [4]. Although copper is a microelement necessary for various vital functions at the same time it is one of the most toxic heavy metals for aquatic organisms (e.g., crustaceans, algae, bacteria) acting adversely already at sub-ppm concentrations [5].

With the aim of controlling copper ions release, a wide variety of organic compounds have been proposed as corrosion inhibitors. They frequently form adsorptive films mediated by electronegative functional groups [6,7]. Unfortunately, the impact of these compounds on the environment is frequently unknown. Some inhibitors may cause reversible (temporary) or irreversible (permanent) damage to living organisms. Their toxicity may manifest either during the synthesis, application or disposal of the compound [8].

In the past two decades many alternative environmentally friendly corrosion inhibitors have been developed. Thus, the research in the field of "green" corrosion inhibitors has been addressed towards the goal of using cheap, effective molecules at low or "zero" environmental impact [9].

In the search of a new strategy natural substances have been considered since most of these substances are safe and can be extracted by simple and cheap procedures. Different plant-extracts-based green inhibitors have recently been proposed as non-toxic corrosion inhibitors. El-Etre et al. [10] found that extract of leaves of henna (*Lawsonia* sp.) acts as a very good corrosion inhibitor for steel, nickel and zinc using polarization techniques. New information on the possible application of the *Ocimum bacilicum* extract and *Ambrosia maritime* as an environmental-friendly aluminum corrosion inhibitors [11,12] as well as the anticorrosive activity of some herb plants frequently used as herbal medicine [13] were provided. Among them, *Thymus vulgaris* extracts (TVE) showed excellent protection for steel, copper and α-brass surfaces [14]. The inhibitory action was attributed to adsorption of these phytochemicals to the metal/solution interface. However, inhibitory action is based on the addition of the inhibitor within the corrosive environment with the purpose of forming an adsorptive protective film on the metal surface.

With the aim of improving the stability of the organic protective films, treatments other than adsorptive films formation were developed. It was shown that phenolic compounds are able to be electropolymerized on metallic surfaces [15,16]. Results showed that polymerized films have perfect adhesion and provided corrosion protection for the metallic materials [15–18].

Considering the above information and with the purpose of attaining an effective eco-friendly corrosion inhibition treatment avoiding the addition of the inhibitor to the surrounding environment, the evaluation of carvacrol (Carv) is reported here. Carv is a natural phenolic derivative component of *Origanum vulgare* and *T. vulgaris* essential oils. Considering its phenolic nature it is interesting to assay possible electrochemical procedures to develop protective polymeric nanolayers.

In order to guarantee the non-toxic characteristics of the new inhibitory strategies toxicological analysis were performed. This is particularly important in case of Carv since this compound not
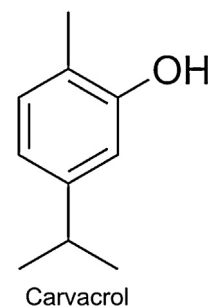

Fig. 1. Chemical structure of carvacrol.

only exhibits beneficial impact due to antioxidant effects at cellular level, but can also induce harmful effects on a large variety of organisms including bacteria, virus, fungi, protozoa, parasites, insects, mollusks, etc [19]. Cytotoxic and morphological changes caused by an organic agent depend on its nature and concentration and on the period in contact with the cells [19].

The aim of this work is to develop an efficient treatment for Cu corrosion that must meet three prerequisites: i) it should be obtained from a natural source; ii) it should not be added to the corrosive solution; iii) the whole treatment should be compatible with the environment.

The performance of Carv both, adsorbed on copper (adCarvCu) or electropolymerized (polyCarvCu), as copper corrosion inhibition treatments were compared. Electrochemical techniques complemented by Attenuated Total Reflectance Fourier Transform Infrared Spectroscopy (ATR-FTIR), X-Ray Photoelectron Spectroscopy (XPS), Scanning Electron Microscopy (SEM) and Atomic Force Microscopy (AFM) surface analyses were used. Cytotoxicity of adCarvCu and polyCarvCu was also assessed to test their compatibility with the biological environment.

2. Materials and methods

2.1. Chemicals

Carvacrol (Carv) (Sigma, St. Louis, MO, USA), which chemical structure is shown in Fig. 1 was used in the experiments. All chemicals used in the assays were of analytical grade and ultrapure water was used to prepare the solutions.

2.2. Cu samples and protection treatments

Cylindrical copper bars (99.7% electrolytic metal copper, 0.9 cm diameter) (Merck, Darmstadt, Germany), whose lateral surfaces were covered with polyoxymethylene, leaving an exposed area of 0.626 cm^2 were used as working electrodes (WE) for electrochemical experiments. Each electrode was mechanically polished with emery paper of different grain sizes using water as lubricant and then washed with water and ethanol, and dried with nitrogen. The electrode surface was carefully observed under optical microscope (Olympus BX51, Olympus Corp., Tokyo, Japan), before and after the experiments, to evaluate possible changes in color and/or texture of copper.

Electrochemical assays were made in a conventional cell with double wall to allow the circulation of water at constant temperature. A platinum foil was used as counter electrode (CE) and a saturated calomel electrode (SCE) as reference electrode. The potential values in the text are referred to the SCE.

Two treatments (adsorption and electropolymerization) were performed to protect Cu samples from corrosion. The adCarvCu was obtained after the immersion for 24 h in a 0.01 M Carv ethanolic
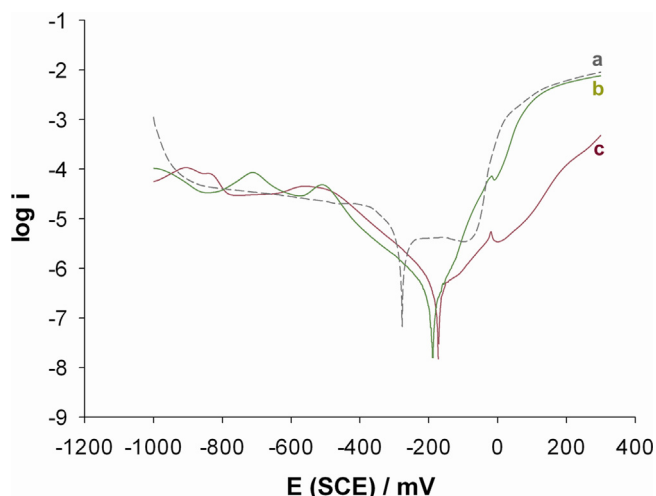
Fig. 2. Polarization curves made in KCl solution (0.136 M), Scan Rate = 1 mVs^{-1} with: (a) (Black) Bare Cu; (b) (Green) Cu + Adsorbed Carv (adCarvCu); (c) (Red) electropolymerized Carv (polyCarvCu). (For interpretation of the references to colour in this figure legend, the reader is referred to the web version of this article.)

solution. In order to obtain a layer of polymerized Carv (polyCarvCu) different procedures were tested. The best results were obtained when polyCarv film was attained by successive cycling the electrode potential at 50 mV s^{-1} (39 cycles) within 0.3 and 1.0 V potential range in 0.1 M Carv, 0.3 M NaOH 70:30 water/ethanol solution. This procedure is a modification of that previously used by Guenbour [20–22] with another phenolic inhibitor. Successive cycling in the 0.3 M NaOH solution and in the ethanolic alkaline solution without Carv was used for comparison. Each test was run in triplicate to verify the reproducibility of the data. In all cases a potentiostat-galvanostat TEQ03 was used.

Cycling between the open circuit potential (OCP) and 0.07 V at 5 mV s^{-1} in 0.136 M KCl solution, with chloride concentration similar to the cell culture medium and other biological media were also made to evaluate the stability of the protective layer.

For biological assays copper disks were obtained from a pure copper sheet (99.7%, 0.1 mm thick and 6 mm diameter) (Merck, Darmstadt, Germany). These disks were washed with (5% v/v) H$_2$SO$_4$, rinsed with ultrapure water and then dried with nitrogen. The polyCarv formation on the disks was carried out as previously described for cylindrical copper samples.

2.3. Measurement of copper ions release

The copper ions released from the disks covered by polyCarv films after their immersion in 3 ml of 0.136 M KCl solution for 3 h, 24 h and 10 days at room temperature was measured by atomic absorption spectroscopy. Flame atomic absorption spectrometer (Shimadzu AA-7000, Kyoto, Japan) was used for the determination of soluble copper concentration, after total dissolution with 1 ml 0.28 M nitric acid. Hollow cathode lamps were used as radiation sources (limit of detection = 0.02 μg/ml, obtained using internal quality control, according to standard procedures).

2.4. Electrochemical tests

Potentiodynamic polarization (Tafel curves) studies were made in 0.136 M KCl in the OCP −0.3 V and OCP to −1.0 V potential ranges at 1 mV s^{-1} scan rate using different electrodes for each assay. The evolution of OCP after the treatments was also measured during

3 h in 0.136 M KCl. Each test was run in triplicate to verify the reproducibility of the data.

2.5. Surface analysis

XPS measurements were performed using Al Kα source (XR50, Specs GmbH) and a hemispherical electron energy analyzed (PHOIBOS 100, Specs GmbH) operating at 40 eV pass energy. A two-point calibration of the energy scale was performed using sputtered cleaned gold (Au 4f7/2, binding energy BE = 84.00 eV) and copper (Cu 2p3/2, BE = 932.67 eV) samples. C 1s at 285 eV was used as charging reference.

ATR-FTIR spectra were obtained in a Varian 660 spectrometer equipped with an attenuated total reflection (ATR) accessory (MIRacle ATR, Pike technologies) with a ZnSe prism. In all cases, each spectrum was the result of 256 scans taken with a resolution of 2 cm^{-1}.

Tapping® mode AFM (Nanoscope V; Bruker, Santa Barbara, CA) in topographic mode was used to characterize the substrates, using silicon tips (ArrowTM NCR; NanoWorld, Neuchâtel, Switzerland) (spring constant, 42 N/m; resonance frequency, 285 kHz). Nanoscope 7.30 and Nanoscope Analyis 1.5 softwares were employed to obtain the images (Bruker).

Scanning electron microscopy (SEM) images of adCarvCu and polyCarvCu were taken using an environmental SEM FEI Quanta 200.

2.6. Biological assays

MC3T3-E1 is an osteoblast precursor cell line derived from *Mus musculus (mouse)*. It was originally obtained from American Type Culture Collection (ATCC) (Rockville, MD, USA). Cells were grown as monolayer in Falcon T-25 flasks with DMEM culture medium (GIBCO-BRL, LA, USA) supplemented with 10% inactivated fetal calf serum (Natocor, Carlos Paz, Córdoba, Argentina), 50 IU/ml penicillin and 50 μg/ml streptomycin sulfate, (complete culture medium: CCM) at 37 °C in a 5% CO$_2$ humid atmosphere. Cells were counted in an improved Neubauer haemocytometer and viability was determined by the exclusion Trypan Blue (Sigma, St. Louis, MO, USA) method; in all cases viability was higher than 95%.

The influence of polyCarv and adCarv films formed on Cu-disks on the viability of the surrounding cells was measured by epifluorescence microscopy after Acridine Orange staining (AO).

For this set of experiments 1×10^6 cells were seeded in Petri dish (10 cm diameter) and grown at 37° C in 5% CO$_2$ humid atmosphere in CCM for 24 h. Then, the medium was removed and a bare Cu disk (according to Section 2.3), polyCarvCu or adCarvCu was added in the center of each Petri dish. Subsequently, fresh medium was incorporated. Cells were grown under these conditions during 24 h. In addition, a cell culture without metal disk was used as negative control. After the exposure period, adherent cells were stained with AO dye (Sigma, St Louis, MO, USA) and immediately after, they were examined by fluorescence microscopy (Olympus BX51, Olympus Corp., Tokyo, Japan) equipped with appropriated filter, connected to an Olympus DP71 (Olympus Corp., Tokyo, Japan) color video camera. The images were taken immediately after opening the microscope shutter to the computer monitor. Surface densities of cells were obtained from digital images using Image-Pro Plus program. Each assay was repeated three times in independent experiments.

For microscopic analyses Petri dishes were divided into three regions (A, B, and C, outer radii = 5 mm, 10 mm and 18 mm, respectively) in order to evaluate the influence of the presence of polyCarv films formed on Cu-disks on cell viability.

Table 1
Electrochemical parameters (Ecorr, icorr and IE%) for bare copper, copper with adsorbed Carv and copper with polyCarv layer.

	Ecorr (mV)	Icorr (uA/cm)	IE%(Icorr)	IE%(100 mV)	IE%(200 mV)	IE%(300 mV)
Bare Cu	−264.2 ± 4.1	4.0 ± 0.7	–	–	–	–
Adsorbed Carv	−179.8 ± 5.9	0.4 ± 0.1	91.0 ± 0.1	21.7 ± 3.2	8.7 ± 0.9	15.3 ± 1.0
polyCarv	−182.0 ± 5.1	0.4 ± 0.1	88.8 ± 2.0	99.7 ± 0.2	98.6 ± 1.1	95.7 ± 1.5

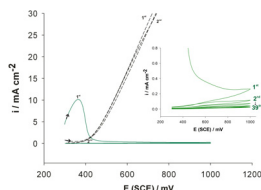**Fig. 3.** First and second voltamperometric cycles made at 50 mV s^{-1} with Cu electrodes in (·····) 0,1 M Carv, 0.3 M NaOH 70/30 H$_2$O/EtOH, (− − − −) Control without Carv. Inset shows the detail of successive cycles made in the presence of 0.1 M Carv.

3. Results

3.1. Electrochemical response of bare Cu and adCarvCu

Polarization curves were recorded in 0.136 M KCl solution using a bare Cu electrode and Cu previously immersed in a 0.1 M Carv solution for 24 h (adCarvCu) (Fig. 2). It can be noticed that the corrosion current (i_{corr}) measured for adCarvCu is lower in nearly one order of magnitude than that of the control. However, adCarvCu showed a sharp increase of current reaching values similar to those of the control at potentials more anodic than E$_{corr}$.

3.2. PolyCarv film formation

With the aim of developing a procedure able to form an electropolymerized layer on copper we assayed different perturbation programs. After several attempts, the electrochemical polymerization of Carv was achieved by successive voltamperommetric cycles carried out in 0.1 M Carv, 0.3 M NaOH 70:30 water/ethanol solution.

During the 1st and 2nd cycles current values of copper in the alkaline electrolyte solution without ethanol (see Supplemental Information Fig. 1S) show a voltamperommetric response similar to that previously reported [23] with a sharp increase of current at potentials more anodic than 0.7 V. In 70:30 ethanol-water solution an abrupt current increase was found at potentials close to 0.4 V, and a nearly linear i/E relationship was recorded (Fig. 3). This important current growth has been previously attributed to the oxidation of ethanol on copper [23–25]. However, if Carv is present in the solution, an anodic contribution was detected at 0.3 V that formed a peak in the 0.3–0.5 V potential range. Subsequently, current decreased sharply and remained very low at potentials higher than 0.5 V and no significant further oxidation was detected. This indicates that the oxidation of Carv on Cu begins at potentials more cathodic than that of ethanol hindering ethanol oxidation. It can be noticed that the largest variations in current density related to Carv oxidation, leading to the passivation of copper surface, were observed during the 1st cycle in the 0.3–0.5 V potential range. An electro-adsorbed layer that leads to polymerization reactions blocking the electrochemically active sites seems to be formed. Upon increasing the number of cycles, current variations became smaller reaching values close to 1 μA/cm^2 after 20 cycles. At the end of 39 cycles the electrode surface was covered by a transparent homogeneous film of polyCarv.
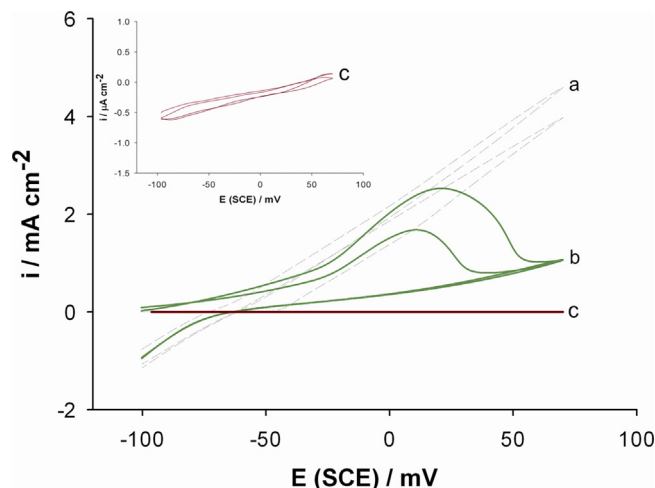

Fig. 4. First and second voltamperometric cycles between the OCP and 0.07 V made in 0.136 M KCl solution with: (a) bare Cu; (b) adsorbed Carv (adCarvCu) and (c) the electropolymerized Carv (polyCarvCu).

3.3. Comparison of protective characteristics of adCarv and polyCarv layers

OCP evolution was evaluated for bare and film-coated Cu electrodes during 3 h in chloride solution. The curves showed a similar potential evolution but OCP values were c.a. 70 mV more anodic in case of samples with polyCarv layer (OCP = −200 mV for bare electrodes and −130 mV for film-coated electrodes).

The Tafel curve for polyCarvCu (Fig. 2) depicted similar cathodic branch and i$_{corr}$ value to those obtained for adCarvCu. However, the anodic branch showed current densities that were up to two orders of magnitude lower than for adCarvCu.

Current Efficiency (IE) values for adCarvCu evaluated at 0.1 V, 0.2 V and 0.3 V decrease to values lower than 20% (Table 1).

IE% was calculated according to:

$$IE\%_{(Ei)} = \frac{i^\circ - i}{i^\circ} \times 100$$

i$^\circ$ is the current density corresponding to bare Cu and i is the current density of the adCarvCu or polyCarvCu measured at Ei = E$_{corr}$, 100 mV, 200 mV or 300 mV.

Unlike adCarvCu, polyCarvCu shows high IE% values at potentials more anodic than E$_{corr}$ (99.7%, 98.6%, and 95.7% for 100 mV, 200 mV and 300 mV, respectively).

The stability of the polyCarv and adsorbed layers was also tested by cycling the electrode in 0.136 M KCl solution in the OCP ±0.07 V potential range. Fig. 4 shows that the current density in case of polyCarv is lower than 1 μA cm^{-2} while current densities three orders of magnitude higher (>2 mA cm^{-2}) were recorded for the bare electrodes and adCarvCu. These results confirm the high stability and inhibitory action of polyCarv and the low protection of adCarv.
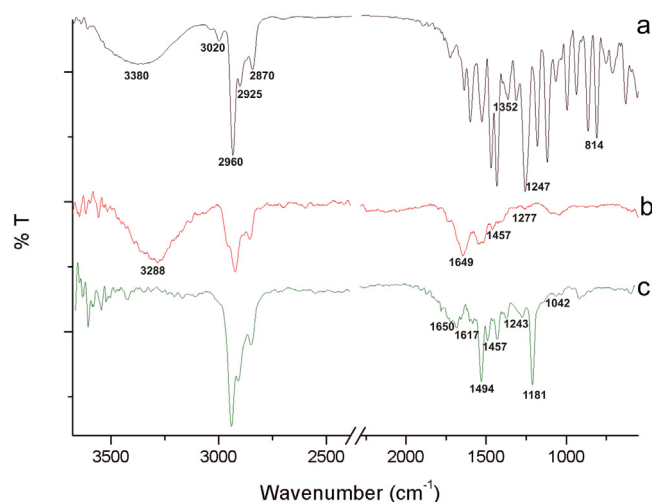
Fig. 5. ATR-FTIR spectrum of (a) Carv (pure drug), (b) adsorbed Carv (adCarvCu) and (c) electropolymerized Carv (polyCarvCu).

3.4. Surface analysis

3.4.1. ATR-FTIR analysis of adCarvCu and polyCarvCu

The infrared spectra of Carv, adCarvCu and polyCarvCu disks are shown in Fig. 5. The ATR-FTIR analysis of the spectra obtained with adCarvCu showed several signals that characterize the spectra of phenol and phenolic derivatives. Among these a contribution at 3288 cm^{-1} (ν(O—H) vibration band) that is accompanied by 1457 (OH in plane deformation vibration), 1277 cm^{-1} (C—OH stretching band) and region band at 1132 and 976 cm^{-1} (C—O stretching vibration) are attributed to OH presence [26,27]. Additionally, peaks at 1649 could be assigned to vibration of quinone structures ((C=O)) [15,27].

Higher transmittance was detected in case of polyCarvCu spectrum with an intense peak at 1181 characteristics of polysustituted phenolic compounds. Peaks at 1494 and 1457 cm^{-1} are assigned to C—C stretching in polysustituted aromatic rings together with the 3044–2800 cm^{-1} band. Importantly, OH contribution at 3300 cm^{-1} characteristic of phenolic groups vanished and the signal of cetonic structures was revealed. Besides, the spectrum shows the signal at 1457 cm^{-1} that corresponds to a C—C stretching vibration. Unlike adCarvCu, peaks at 1243, 1494, 1617 and 1042 cm^{-1} were detected for polyCarvCu and can be assigned to ether bonds for phenolic derivatives [26,27]. In agreement, in previous works [15,28] signals in the 1220–1242 cm^{-1} range were assigned to ether bonds. Interestingly, the contribution at 1650 cm^{-1} is associated to cetone bonds, indicating a probable oxidation of the organic compound to a quinone structure.

3.4.2. XPS analysis of adCarvCu and polyCarvCu

XPS spectra show that the C/Cu ratio for pristine substrate is greater than for the adCarvCu sample. It must be taken into account that this adCarvCu sample was obtained after the immersion of a pristine substrate in the Carv-containing solution for 24 h. Thus, the lower C/Cu ratio can be explained by a nearly complete or fully complete replacement of the original adventitious C by Carv, indicating a stronger Carv interaction with the original substrate.

The Cu2p region of the photoelectron spectra for adCarvCu and polyCarvCu (Fig. 6A) shows the typical Cu^{+2} shake up satellites at higher binding energies than the characteristic Cu2p3/2 line. The adCarvCu shows sharper peaks for Cu2p3/2 and Cu2p1/2 than for polyCarvCu. PolyCarvCu (with an organic layer thicker than that of adCarvCu) shows a relatively enhanced shake up satellite. The copious organic layer obtained on the Cu surface by elec-

tropolymerization, probably attenuates the underneath metallic photoelectron signal. Therefore mostly the Cu-polyCarv interface shapes Cu2p signal in polyCarvCu (Fig. 6A polyCarvCu).

In adCarvCu spectrum three components at the C1s signal were fitted (Fig. 6B). The first one at 284.8 eV attributed to C—C and C—H [29–32]. The second one at 285.8 eV may be assigned to the phenolic C—O bond (C(ph)—O) [29–31,33]. Finally a third component at 288.0 eV is close to that associated to C=O, that is carboxyl-quinone group [29,31,33,34].

Similarly, for polyCarvCu samples (Fig. 6C), the C1s was fitted with three components (Fig. 6C): the first two at 284.7 eV and 285.5 eV were attributed to (C—C; C—H) and C(ph)—O, respectively. A third contribution at 291.1 eV, is due to the $\pi \geq \pi^*$ shake up satellite of the aromatic structure. Considering that it is absent in case of adCarvCu it could be inferred that there is a higher number of Carv molecules on Cu surface with polyCarvCu than in the case of adCarvCu. Several authors also include a fourth contribution at 286.8 eV that could be attributed to C carboxyl-quinone group [29,31,33,34].

On the other hand, O1s spectra for adCarvCu and bare Cu showed a contribution at 533.7 eV that may be assigned to several oxygen-containing species such as H$_2$O adsorbed on Cu [35,36]. The polyCarvCu showed widening with the concomitant increase in the peak area at 533.7 eV. It could be associated to a higher concentration of several oxygen-containing species such as those with ether bonds [20,32,37]. Additionally, both, polyCarvCu and adCarvCu, showed wide bands at 531.6 and 530.8 eV respectively that could be assigned to C—O*, C=O or C—O-Me (Me = metal) [20,37].

3.4.3. SEM and AFM imaging

SEM images (Fig. 7a) show the surface morphology of polyCarvCu after the cycling process (39 cycles). It can be noticed that polyCarv film looks very smooth and homogeneous at a high magnification (X40000) with loosely perceptible cracks due to dehydration process that takes place in the vacuum environment necessary for SEM observations. Unlike polyCarv layer, adCarv film additionally includes aggregates of globules. AFM images at higher magnification show (Fig. 7b) closed packed morphology of polyCarvCu that fully covered the Cu surface where small round flakes can be distinguished. The line profile of the AFM image and the statistical analysis revealed that these particles are very small, less than 5 nm height in case of polyCarv and several times larger (18 nm height) in case of adCarv. Roughness parameters are included in the figure revealing the higher roughness of the adCarv layer (Ra = 9.1 for adCarv and Ra = 3.3 for polyCarv).

3.5. Measurement of copper released by atomic absorption spectroscopy

The concentrations of copper ions released by copper disk with and without the electropolymerization treatment, during 24 h in 0.136 M KCl solution measured by atomic absorption spectroscopy show values around $21.8 \pm 5.2\ \mu g\ cm^{-2}$ for bare Cu and $2.6 \pm 0.7\ \mu g\ cm^{-2}$ for polyCarvCu. Results of assays with adCarvCu were more scattered than the others but in all cases copper release was at least 8 times higher than that of polyCarv. Thus, copper ions release measurements showed a trend similar to that shown in electrochemical experiments of Fig. 4.

3.6. Biological assays

The toxicity of copper ions and organic products released by the treated disks was evaluated by viability assays (AO) previously described. Fig. 8 shows the percentage of living cells in each region after 24 h exposure to Cu, adCarvCu and polyCarvCu disks. According to our previous work, the reduction of cell viability in the
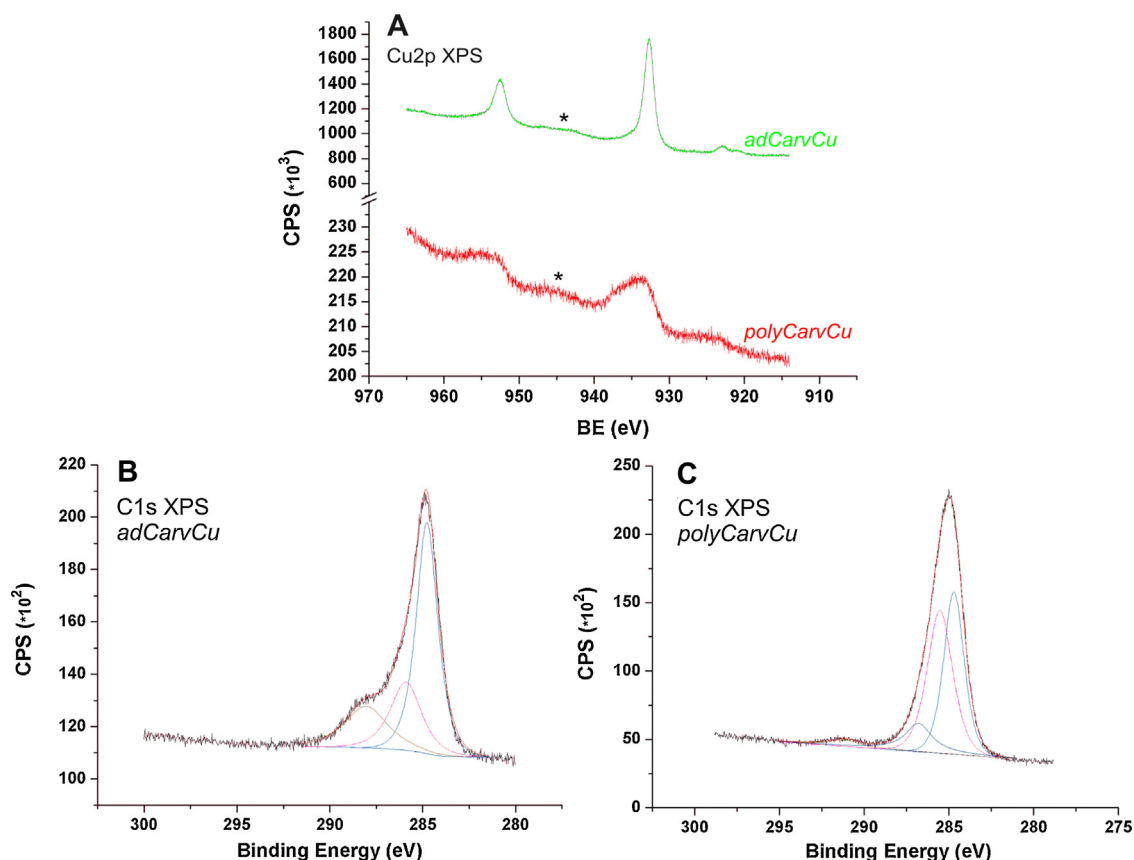
Fig. 6. XPS spectra. A: Cu2p spectra for adsorbed Carv (adCarvCu) and electropolymerized Carv (polyCarvCu); B: C1s spectrum for adCarvCu; C: C1s spectrum for polyCarvCu.

presence of bare Cu disk is very high near the metal (region A) and decreases with the distance from the metal surface in agreement with previous results [38] (significant decrease in all the tested regions, $p \leq 0.001$ to control). Conversely, polyCarvCu disks were well tolerated by the cells around the disk, thus, cell viability was close to that of the control without Cu disk in all the regions. In case of adCarvCu the viability was close to the control (without disk) only in region C, far from the disk. However, at shorter distance (Regions A and B) viability was close to bare Cu (less than 30%, in case of Region A).

4. Discussion

4.1. Copper corrosion and copper ions release

Copper is one of the most toxic heavy metals for aquatic systems. Copper release is induced by the adsorption of chloride ions to the surface with the subsequent formation of $CuCl_2^-$ complex. According to Kear et al. [2]:

$$Cu + Cl^- \leftrightarrow CuCl_{ad} \tag{1}$$

$$CuCl_{ad} + Cl^- \leftrightarrow CuCl_2^- \tag{2}$$

$$O_2 + 2H_2O + 4e^- \leftrightarrow 4OH^- \tag{3}$$

Then the hydrolysis of a CuCl deposit into a porous layer of Cu_2O occurs which further hydrolyzes to form a top layer of atacamite

$$2CuCl + H_2O \leftrightarrow Cu_2O + 2H^+ + 2Cl^- \tag{4}$$

$$Cu_2O + Cl^- + 2H_2O \leftrightarrow Cu_2(OH)_3Cl + H^+ + 2e^- \tag{5}$$
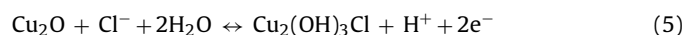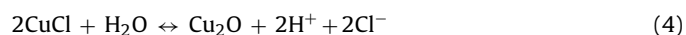
It is widely accepted that the release of copper in chloride solutions is under mass transport control. It was concluded that the

limiting step is the movement of cuprous chloride complex away from the electrode surface to the bulk solution [2].

4.2. Corrosion inhibition by adCarv and polyCarv layers

Many organic compounds have been proposed to inhibit the dissolution by forming an adsorptive film on the copper surface able to limit copper ions diffusion, some of them with hetero-cycles compounds [6,7,39]. Recently, new derivatives were designed (triazolyl-acylhydrazone and 1,2,4 triazol derivatives) to form adsorptive films that were tested in inhibitor-containing solutions [1,40,41]. The decrease in copper dissolution is achieved by forming a thin layer that covers the active sites hindering the formation of cuprous chloride, cuprite and atacamite. Their inhibition efficiency increased with time of immersion in the inhibitor-containing solution and with inhibitor concentration up to its maximum solubility in aqueous solution [40].

The election of a suitable inhibition treatment for a particular application is complex. The final choice of the inhibitor for a particular application is restricted by two factors: increased environmental awareness and the need to promote environmentally friendly processes. New environmental regulations requires the replacement of toxic compounds with the so called "Green chemicals" [42]. However, the compatibility of the inhibitor with the environment is rarely evaluated when a new designed compound is proposed. On the other hand, some treatments require an inhibitor-containing solution to avoid the progressive decrease in their efficacy; these treatments are not suitable for several systems that do not allow the use of inhibitors within the corrosive solution (biological fluids for medical applications, solutions that must be wasted to the neighboring environment).
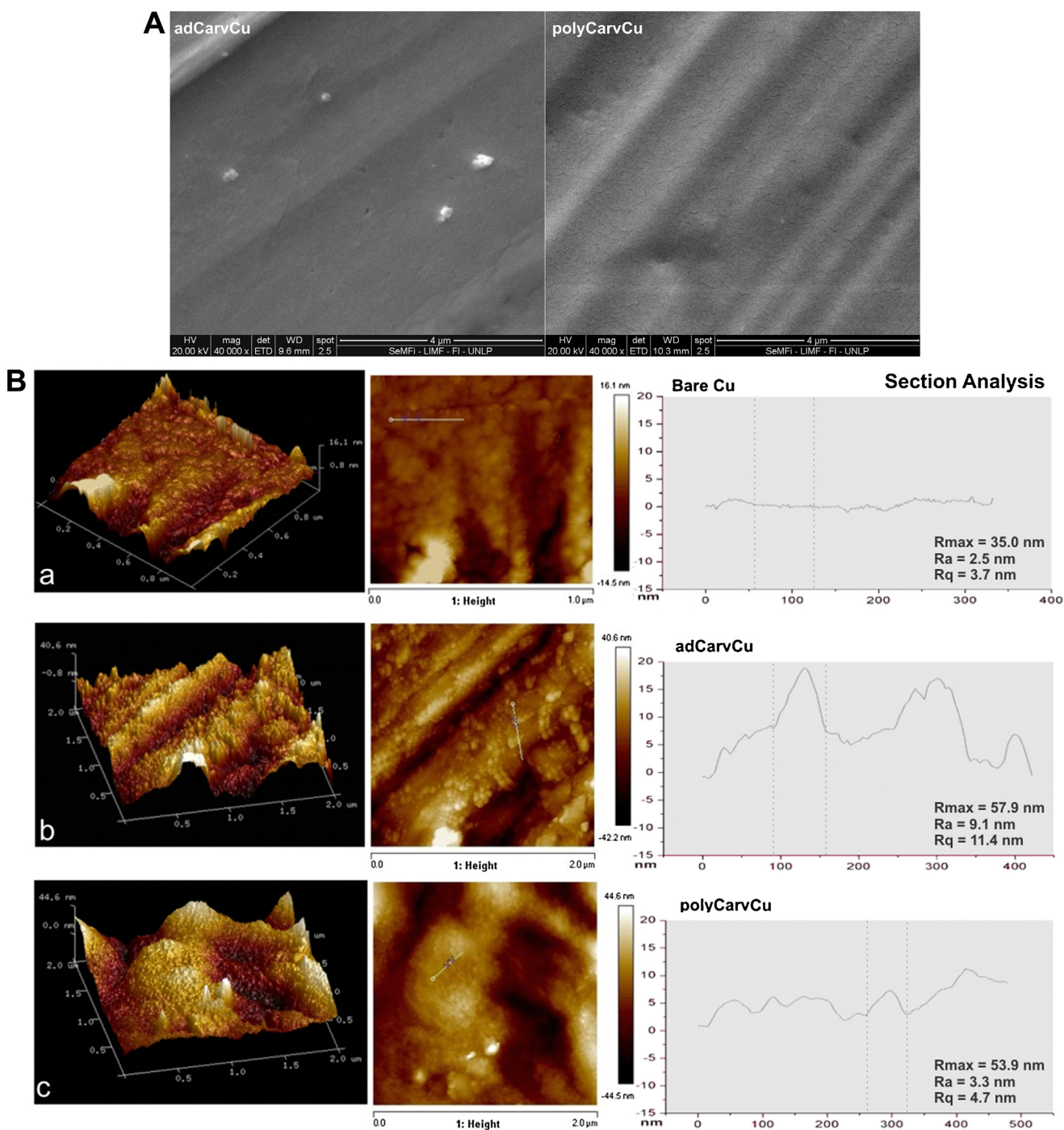
Fig. 7. (A) SEM images of the adCarvCu and polyCarv layers formed on Cu surface (polyCarvCu). Aggregates of globules can be seen on adCarvCu. (B) AFM images corresponding to Bare Cu (a), adsorbed Carv (adCarvCu); (b) and electropolymerized Carv layer formed on Cu surface (polyCarvCu) (c). Section analyses are shown on the left.

Considering these restrictions Carv, a natural compound (component of origanum and thymus) was used and treatments with zero environmental impact were designed. These treatments consist in (i) formation of an adsorptive layer previous to the immersion in the corrosive solution (adCarvCu) and, (ii) development of electropolymerized layer (polyCarvCu).

Electrochemical tests revealed that i_{corr} measured for adCarvCu were close to one order of magnitude lower than the control without treatment. Unfortunately, the adsorptive layer was not stable and during the anodic polarization and after voltamperometric cycling in a chloride solution (within a potential range close to the OCP value) the molecules were desorbed. Thus, the successive cycles of adCarvCu in the corrosive medium without Carv showed the increase of current indicating that the passivating action decreased due to this processes. In agreement, polarization curves showed very low IE values for potentials more anodic than the corrosion potential.

As a second strategy, potential cycling was tested with the aim of polymerizing Carv on Cu surface. Fig. 3 shows that during the first cycle there is a peak in the 0.3–0.5 V that is absent in the control and can be attributed to the oxidation/polymerization of Carv on the copper surface. According to ATR-FTIR and XPS results the oxidation products kept on the surface blocking the active sites. This is connected with the sharp decrease in current density and
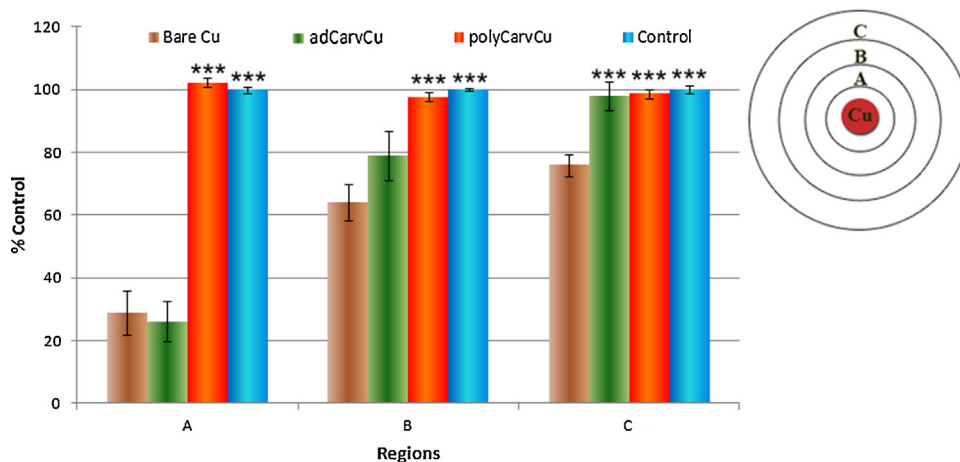
Fig. 8. Viability of cells (% of the Control value) by Acridine Orange staining after 24 h exposure to: bare Cu disk, adsorbed Carv (adCarvCu) disk, electropolymerized Carv (polyCarvCu) disk and control without disk. Different regions A,B,C were analyzed to evaluate the variation of the number of cells with the distance from Cu disk. Significant difference (***, $p \leq 0.001$) with respect to bare Cu at the corresponding region.

subsequently, during the following cycles, to the very low current values related to the growth of the protective layer.

Unlike adCarvCu, the polyCarvCu layer was very stable in chloride solutions without Carv since current density values in the order of $\mu A\,cm^{-2}$ were recorded during cycling at potentials more anodic than OCP. Our results show that the polymerization process for polyCarvCu is similar to that found with some phenolic derivatives [43]. It is believed [15] that the polymers formed from substituted phenols are more passivating than the polymers obtained from phenol, which may be associated with effects from the substituting in the phenolic structure. It is widely accepted that the decrease of oxidation current density during the successive cycles and the lack of reduction peaks in the reverse scan confirm the blockage of the electrode surface due to the formation of the electropolymerized layer [15,27,43]. This layer is able to deactivate the electrode surface by hindering the diffusion of the copper-chloride complexes to the bulk solution or the removal of products from the active sites and interfering with the supply of fresh reactants from the bulk solution (see Eqs. (1)–(5)).

It has been reported that the electropolymerization of phenolic structures such as cresol, begins with deprotonation of the phenyl functional group and the formation of the phenoxy radical, or the molecule can react with another molecule to give predominantly a para-linked dimeric radical. Further oxidation of radicals may lead to a neutral dimmer that may be further oxidized creating oligomers to polymers [27]. In this way an insoluble polyphenolic layer is formed. According to XPS and ATR-FTIR data, the polymerization of Carv involves a mechanism similar to that of cresol.
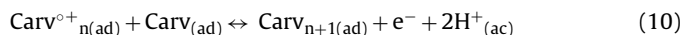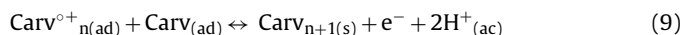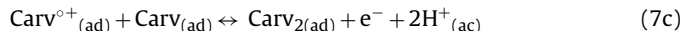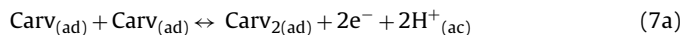
The comparison of ATR-FTIR and XPS surface analysis of adCarvCu and polyCarvCu shows that different bonds are formed on copper surfaces. Adsorbed layer leads to the formation of cetonic structures within a thin layer that partially inhibit the dissolution process. Results of XPS spectra indicate that there is a strong interaction of adsorbed Carv molecules with the surface evidenced by the characteristic signals of phenol which are higher than those of the polymeric structures. It has been reported that adsorption geometry changes with potential and parallel or vertical orientation of the ring may be found according to the potential value and concentration of the phenolic molecule [27].

On the other hand, ATR-FTIR shows ether bonds for PolyCarv confirming the presence of polyether layer in agreement with results related to the polymerization of other phenolic derivatives [15,27]. A shiny and uniform layer was observed with naked eye on

polyCarvCu surface. AFM images showed round flakes close to 5 nm height on this surface. Larger surface irregularities were observed in the section profile and in SEM images in case of adCarvCu.

4.3. Electropolymerization mechanism

Results showed that the anodic current density recorded at potentials ≥ 0.5 V in the ethanolic solution without Carv could be associated to EtOH oxidation on Cu surface. However, in the presence of Carv, at more cathodic potentials, Carv oxidized on Cu blocking the surface with the oxidation products that were detected by ATR-FTIR and XPS analysis. Interestingly, the inhibition was probably so strong that no particular signals related to EtOH oxidation were detected in the analysis. A mechanism to interpret these complex oxidation processes is proposed here and was adapted from Garfias-García et al. [44] involving the reactions shown below. Initially, the molecules adsorbed on the metal surface (Reaction (6)) and heterogeneous reactions take place at the electrode-solution interface. These adsorbed molecules are probably associated to the ATR-FTIR contribution in the region close to $3300\,cm^{-1}$. Subsequently, they may be oxidized and form dimmers in one or two steps (Reactions (7a)–(7c)).

$$Carv \leftrightarrow Carv_{(ad)} \tag{6}$$

$$Carv_{(ad)} + Carv_{(ad)} \leftrightarrow Carv_{2(ad)} + 2e^- + 2H^+_{(ac)} \tag{7a}$$

$$Carv_{(ad)} \leftrightarrow Carv^{\circ+}_{(ad)} + e^- \tag{7b}$$

$$Carv^{\circ+}_{(ad)} + Carv_{(ad)} \leftrightarrow Carv_{2(ad)} + e^- + 2H^+_{(ac)} \tag{7c}$$

$$Carv_{n(ad)} \leftrightarrow Carv^{\circ+}_{n(ad)} + e^- \tag{8}$$

$$Carv^{\circ+}_{n(ad)} + Carv_{(ad)} \leftrightarrow Carv_{n+1(s)} + e^- + 2H^+_{(ac)} \tag{9}$$

$$Carv^{\circ+}_{n(ad)} + Carv_{(ad)} \leftrightarrow Carv_{n+1(ad)} + e^- + 2H^+_{(ac)} \tag{10}$$

In Reaction (8) $Carv^{\circ+}_{n(ad)}$ is an adsorbed radical cation oligomer resulting from the oxidation of the oligomer $Carv_{n(ad)}$ which further oxidation leads to $Carv_{n+1(ad)}$ (Reaction (10)) and in case of adsorption treatment leads to $Carv_{n+1(s)}$ (Reaction (9)) that may result in the formation of aggregates on the surface (see Fig. 7a).

At potentials near 400 mV it seems that the adsorbed molecules and oligomers can be quickly assembled into an ordered layer leading to a very compact and highly protective transparent film of polyCarv that inhibits further oxidation.

4.4. Biological response

In order to evaluate the toxicity of the treatments cytotoxicity assays were performed and revealed a correlation between copper ions release and the biological response. Thus, high cytotoxicity was found for copper without treatment in agreement with the results of similar assays made with copper in different chloride-containing media [45–47]. A less toxic effect was found in the case of adCarvCu, particularly at longer distance from the copper ions source. Conversely, polyCarvCu showed very good tolerance by the cells. It is known that the concentration of ions close to the bare copper disks is higher than at further distance and the cell viability is lower close to the bare disk [47]. Interestingly, our results showed that the viability is distance-dependent not only for Cu without treatment but for adCarv as well.

Electrochemical experiments made with bare copper, adCarvCu and polyCarvCu (Fig. 4) show that current densities for polyCarvCu are three orders of magnitude lower than that of the bare electrodes and adCarvCu at +300 mV. Consequently, the release of copper ions should be higher in case of bare copper and adCarv layer. In fact, the concentration of copper ions measured by atomic absorption spectroscopy after 24 h immersion at OCP in the 0.136 M KCl solution was at least 8 times lower for polyCarv than for bare samples and adCarv. In earlier works [45,47] we studied the dependence of cells viability with copper ions released by copper metal samples and results demonstrated that concentration and distance from the source of ions were inversely proportional. Since experimental results presented here showed that the cell viability is markedly higher in case of polyCarvCu samples than for adCarvCu and bare copper it can be inferred that viability results are also inversely related with the concentration of copper ions release. Besides, considering that viability of cells exposed to the control without copper disk and polyCarvCu are similar, it could also be concluded that polyCarv layer is not toxic for the surrounding cells.

Importantly, polyCarvCu maintains a low level of copper concentration able for medical purposes (contraception in case of intrauterine devices) or for environmental purposes.

5. Conclusions

Two eco-friendly strategies (adCarvCu and polyCarvCu) were designed to be tested with the aim of reducing the release of copper in the environment. Adsorptive layer (adCarvCu) that contains cetonic structures detected by ATR-FTIR did not fulfill the requirements since it was not effective enough to inhibit copper ions release. The electrochemical tests showed that the protective characteristics were lost at potentials slightly more anodic than the corrosion potential.

PolyCarvCu was obtained by an anodic electropolymerization process. The coating showed a good adherence and protective properties up to 0.3 V. The growing process probably involves the deprotonation of the molecules followed by the electropolymerization reactions. In this process, the polymerization affects the —OH groups by formation of quinonic structures and ether bonds (—OH signal disappears).

The shielding character of the coating provides an excellent protective action to this layer inhibiting the corrosion process and, consequently, the release of copper ions to the aqueous medium.

Cytotoxicity assays showed that viability of cells decreased in case of adCarvCu but it was not significantly affected by polyCarvCu. Thus, the reduction in copper ions release and the non-toxic properties of this polymeric layer obtained from a natural phenolic derivative guarantee the reduction of toxicity by copper in the surrounding cells.

Consequently, polyCarvCu strategy is able to satisfy the eco-friendly prerequisites since it is obtained from a natural source (*O. vulgare*) and is a non toxic corrosion protective treatment. Importantly, it is able to inhibit the release of copper avoiding the addition of the inhibitor to the corrosive solution, which is an advantage for medical and environmental applications.

Acknowledgements

Appendix A. Supplementary data

Supplementary data associated with this article can be found, in the online version, at http://dx.doi.org/10.1016/j.jhazmat.2016.03.086.

References

[1] H. Tian, Y.F. Cheng, W. Li, B. Hou, Triazolyl-acylhydrazone derivatives as novel inhibitors for copper corrosion in chloride solutions, Corros. Sci. 100 (2015) 341–352.

[2] G. Kear, B.D. Barker, F.C. Walsh, Electrochemical corrosion of unalloyed copper in chloride media. A critical review, Corros. Sci. 46 (2004) 109–135.

[3] M. Shahid, Corrosion protection with eco-friendly inhibitors, Adv. Nat. Sci. Nanosci. Nanotechnol. 2 (2011) 1–6.

[4] I. Vopálenská, L. Váchová, Z. Palková, New biosensor for detection of copper ions in water based on immobilized genetically modified yeast cells, Biosens. Bioelectron. 72 (2015) 160–167.

[5] A. Käkinen, O. Bondarenko, A. Ivask, A. Kahru, The effect of composition of different ecotoxicological test media on free and bioavailable copper from CuSO$_4$ and CuO nanoparticles: comparative evidence from a Cu-selective electrode and a Cu-biosensor, Sensors (Basel) 11 (2011) 10502–10521.

[6] Y.C. Pan, Y. Wen, R. Zhang, Y.Y. Wang, Z.R. Zhang, H.F. Yang, Electrochemical and SERS spectroscopic investigations of 4-methyl-4H-1,2,4-triazole-3-thiol monolayers self-assembled on copper surface, Appl. Surf. Sci. 258 (2012) 3956–3961.

[7] Sudheer, M.A. Quraishi, Electrochemical and theoretical investigation of triazole derivatives on corrosion inhibition behavior of copper in hydrochloric acid medium, Corros. Sci. 70 (2013) 161–169.

[8] M.M. Antonijevic, M.B. Petrovic, Copper corrosion inhibitors. A review, Int. J. Electrochem. Sci. 3 (2008) 1–28.

[9] G. Moretti, F. Guidi, G. Grion, Tryptamine as a green iron corrosion inhibitor in 0.5 M deaerated sulphuric acid, Corros. Sci. 46 (2004) 387–403.

[10] A.Y. El-Etre, M. Abdallah, Z.E. El-Tantawy, Corrosion inhibition of some metals using lawsonia extract, Corros. Sci. 47 (2005) 385–395.

[11] E.E. Oguzie, A.I. Onuchukwu, P.C. Okafor, E.E. Ebenso, Corrosion inhibition and adsorption behaviour of *Ocimum basilicum* extract on aluminium, Pigment Resin Technol. 35 (2006) 63–70.

[12] A.M. Abdel-Gaber, E. Khamis, H. Abo-ElDahab, S. Adeel, Inhibition of aluminium corrosion in alkaline solutions using natural compound, Mater. Chem. Phys. 109 (2008) 297–305.

[13] E. Khamis, N. AlAndis, Herbs as new type of green inhibitors for acidic corrosion of steel, Materwiss. Werksttech. 33 (2002) 550–554.

[14] A.S. Fouda, K. Shalabi, A.A. Idress, *Thymus vulgarise* extract as nontoxic corrosion inhibitor for copper and α—brass in 1 M HNO$_3$ solutions, Int. J. Electrochem. Sci. 9 (2014) 5126–5154.

[15] M. Ferreira, H. Varela, R.M. Torresi, G. Tremiliosi-Filho, Electrode passivation caused by polymerization of different phenolic compounds, Electrochim. Acta 52 (2006) 434–442.

[16] L.G. Andión, P. Garcés, R. Lapuente, J.L. Vázquez, F. Cases, Corrosion behaviour at the interface of steel bars embedded in cement slurries effect of phenol polymer coatings, Corros. Sci. 44 (2002) 2805–2816.

[17] J.R. Santos, L.H.C. Mattoso, A.J. Motheo, Investigation of corrosion protection of steel by polyaniline films, Electrochim. Acta 43 (1998) 309–313.

[18] I. Sekine, K. Kohara, T. Sugiyama, M. Yuasa, Syntheses of polymerized films on mild steels by electro-oxidation and electroreduction and their corrosion resistance, J. Electrochem. Soc. 401 (1992) 3090–3097.

[19] F. Bakkali, S. Averbeck, D. Averbeck, M. Idaomar, Biological effects of essential oils—a review, Food Chem. Toxicol. 46 (2008) 446–475.

[20] A. Guenbour, A. Kacemi, A. Benbachir, L. Aries, Electropolymerization of 2-aminophenol. Electrochemical and spectroscopic studies, Prog. Org. Coat. 38 (2000) 121–126.

[21] A. Guenbour, A. Kacemi, A. Benbachir, Corrosion protection of copper by polyaminophenol films, Prog. Org. Coat. 39 (2000) 151–155.

[22] G. Mengoli, M.M. Musiani, An overview of phenol electropolymerization for metal protection, J. Electrochem. Soc. 134 (1987) 643C–652C.

[23] T.R.L.C. Paixão, D. Corbo, M. Bertotti, Amperometric determination of ethanol in beverages at copper electrodes in alkaline medium, Anal. Chim. Acta 472 (2002) 123–131.

[24] M.R. Othman, J. Salimon, Analysis of ethanol using copper and nickel sheet, Malays. J. Anal. Sci. 11 (2007) 379–387.

[25] W. Novakowski, M. Bertotti, T.R.L.C. Paixão, Use of copper and gold electrodes as sensitive elements for fabrication of an electronic tongue: discrimination of wines and whiskies, Microchem. J. 99 (2011) 145–151.

[26] S.R. Laboratories, W.W. Simons, The Sadtler Handbook of Infrared Spectra, Sadtler Research Laboratories, Philadelphia, 1978.

[27] M. Gattrell, D.W. Kirk, A Fourier Transform Infrared Spectroscopy study of the passive film produced during aqueous acidic phenol electro-oxidation, J. Electrochem. Soc. 139 (1992) 2736–2744.

[28] L. Bao, R. Xiong, G. Wei, Electrochemical polymerization of phenol on 304 stainless steel anodes and subsequent coating structure analysis, Electrochim. Acta 55 (2010) 4030–4038.

[29] J.L. Solomon, R.J. Madix, J. Stöhr, Orientation and absolute coverage of benzene aniline, and phenol on Ag(110) determined by NEXAFS and XPS, Surf. Sci. 255 (1991) 12–30.

[30] H. Ihm, J.M. White, Stepwise dissociation of thermally activated phenol on Pt(111), J. Phys. Chem. B 104 (2000) 6202–6211.

[31] P. Krawczyk, J.M. Skowroński, Multiple anodic regeneration of exfoliated graphite electrodes spent in the process of phenol electrooxidation, J. Solid State Electrochem. 18 (2014) 917–928.

[32] S. Sundaram, S.K. Annamalai, Selective immobilization of hydroquinone on carbon nanotube modified electrode via phenol electro-oxidation method and its hydrazine electro-catalysis and *Escherichia coli* antibacterial activity, Electrochim. Acta 62 (2012) 207–217.

[33] Z.R. Yue, W. Jiang, L. Wang, S. Gardner, C.U. Pittman Jr., Surface properties of electrochemically oxidized carbon fibers, Carbon N. Y. 37 (1999) 1797–1807.

[34] M. Gattrell, D.W. Kirk, A study of electrode passivation during aqueous phenol electrolysis, J. Electrochem. Soc. 140 (1993) 903–911.

[35] Y. Ávila-Torres, L. Huerta, N. Barba-Behrens, XPS-characterization of heterometallic coordination compounds with optically active ligands, Hindawi Publ. Corp. J. Chem. 2013 (2013) 1–9.

[36] W. Zhang, H. Zhang, J. Xiao, Z. Zhao, M. Yu, Z. Li, Carbon nanotube catalysts for oxidative desulfurization of a model diesel fuel using molecular oxygen, Green Chem. 16 (2014) 211–220.

[37] R. Lapuente, C. Quijada, F. Huerta, F. Cases, J.L. Vázquez, X-ray Photoelectron Spectroscopy study of the composition of polyphenol films formed on Pt by electropolymerisation of phenol in the presence of sulphide in carbonate medium, Polym. J. 35 (2003) 911–919.

[38] C.A. Grillo, M.L. Morales, M.V. Mirífico, M.A. Fernández Lorenzo, Synergistic cytotoxic effects of ions released by zinc-aluminum bronze and the metallic salts on osteoblastic cells, J. Biomed. Mater. Res. A 101 (2013) 2129–2140.

[39] S.M. Milić, M.M. Antonijević, Some aspects of copper corrosion in presence of benzotriazole and chloride ions, Corros. Sci. 51 (2009) 28–34.

[40] Z. Khiati, A.A. Othman, M. Sanchez-Moreno, M.C. Bernard, S. Joiret, E.M.M. Sutter, et al., Corrosion inhibition of copper in neutral chloride media by a novel derivative of 1,2,4-triazole, Corros. Sci. 53 (2011) 3092–3099.

[41] C.A. Grillo, M.V. Mirífico, M.L. Morales, M.A. Reigosa, M.A. Fernández Lorenzo, Assessment of cytotoxic and cytogenetic effects of a 1,2,5-thiadiazole derivative on CHO-K1 cells. Its application as corrosion inhibitor, J. Hazard. Mater. 170 (2009) 1173–1178.

[42] R.M. Palou, O. Olivares-Xomelt, N.V. Likhanova, in: M. Aliofkhazraei (Ed.), Protection, InTech, 2014, pp. 257–303, Chapter 19.

[43] G. Bereket, B. Duran, Anticorrosive properties of electrosynthesized poly(m-aminophenol) on copper from aqueous phenylphosphonic acid solution, Prog. Org. Coat. 64 (2009) 57–66.

[44] E. Garfias-García, M. Romero-Romo, M.T. Ramírez-Silva, J. Morales, M. Palomar-Pardavé, Mechanism and kinetics of the electrochemical formation of polypyrrole under forced convection conditions, J. Electroanal. Chem. 613 (2008) 67–79.

[45] C.A. Grillo, M.A. Reigosa, M.A. Fernández Lorenzo, Effects of copper ions released from metallic copper on CHO-k1 cells, Mutat. Res. Toxicol. Environ. Mutagen. 672 (2009) 45–50.

[46] F. Alvarez, C.A. Grillo, P. Schilardi, A. Rubert, G. Benítez, C. Lorente, et al., Decrease in cytotoxicity of copper-based intrauterine devices (IUD) pretreated with 6-mercaptopurine and pterin as biocompatible corrosion inhibitors, ACS Appl. Mater. Interfaces 5 (2013) 249–255.

[47] M.D. Pereda, M. Reigosa, M.A. Fernández Lorenzo, Relationship between radial diffusion of copper ions released from a metal disk and cytotoxic effects. Comparison with results obtained using extracts, Bioelectrochemistry 72 (2008) 94–101.